RATE AS A FUNCTION OF CATALYST GEOMETRY

The influence of the geometry of reduced and reduced-and-nitrided, fused-ammonia synthesis catalyst on rate of the Fischer-Tropsch reactions was studied by varying (1) the particle size, (2) the extent of reduction, and (3) the reduction temperature (*54*). Catalytic activity and composition changes were determined for all three series. In this section the data are interpreted by simple computations, and in a subsequent section a special solution of the differential equations of Wheeler is applied.

EFFECT OF PARTICLE SIZE, TEMPERATURE OF REDUCTION, AND EXTENT OF REDUCTION

These tests employed our standard fused-iron oxide catalyst D3001, containing, in weight-percent, Fe 67.4; MgO, 4.61; K_2O, 0.57; SiO_2, 0.71; and Cr_2O_3, 0.65. The original material of about 4- to 8-mesh was crushed in a roller mill and sieved into the desired size fractions. The catalyst was reduced in hydrogen at temperatures varying from 400° to 625° C, as desired, in a metal block reactor (*9*) and for nitrided catalysts the sample was subsequently treated with ammonia at 350° C in this unit. The catalyst-testing units and mode of operation have been described on pages 4 and 5 and in previous papers (*7*, *9*).

Tests were made with $1H_2+1CO$ gas at 21.4 atmospheres with the space velocity held at about 300 hr^{-1}, and the temperature of the reactor varied to maintain the apparent CO_2-free contraction at about 65 percent. The activity in terms of volume of synthesis gas reacted per hour per gram of iron at 240° C was computed by empirical rate equation (13), with the activation energy taken as 19 kcal/mole. Experiments at a constant temperature with the flowrate varied to maintain a constant conversion would have been preferable; however, this type of experiment would require more than fivefold variations of total gas conversion, and localized overheating of the catalyst probably would have occurred at the higher space-time yields. Although the use of an empirical equation with a constant energy of activation (*8*) is incorrect, fortunately the errors introduced do not change the interpretation of the results, as will be shown in the next section. Reproducibility of catalytic activity as computed by the empirical equation was fairly good, as shown by duplicate tests of nitrided catalysts:

Mesh size:	*Average activity per gram Fe for weeks 2–6*
6–8	75
	77
42–60	207
	222

Condensed products from the synthesis were divided into several fractions by simple one-plate distillation (*9*). The reproducibility of product characterizations was less satisfactory, and these data are used only to show major trends.

In some experiments a sizable fraction of the catalyst disintegrated into finer particles during the pretreatment. On this basis the pretreated catalysts for the particle-size series were sieved to the desired mesh size under liquid heptane. Suitable precautions were taken to preclude oxidation of the catalyst in this manipulation. When this procedure was adopted, the extent and temperature of reduction series was nearly completed; however, a few additional experiments with catalysts sieved after pretreatment were made to show that the trends observed in the earlier tests were essentially correct.

It was desired to select a value for activity at a suitable period after steady conditions were attained. The activity was somewhat erratic in the first 2 or 3 days of synthesis, but in the remaining period of synthesis the activity was relatively constant. The deviations (absolute) of the average activities of the second to sixth week from the activity in the second week averaged only 6 percent for all tests considered. On this basis the average value for the second to sixth weeks was used as an expression of activity.

In subsequent considerations the particles will be assumed to be smooth spheres. A hypothetical spherical radius was computed from the average weight per particle of raw catalyst and the real density of this material. It is further assumed that the pore geometry of the pretreated catalyst may be used in activity correlations, despite the fact that these catalysts are oxidized to a large extent during synthesis (*4*, *55*). Subsequent sections considering reaction and mass transport in pores and oxidation of catalyst largely justify this postulate.

The three groups of experiments for both

reduced and reduced-and-nitrided samples are reported:

A.—*Particle size series:* The first group of catalysts was virtually completely reduced at 450° C and sieved after pretreatment. Catalysts of 6- to 8-mesh and 28- to 32-mesh were tested after reduction at 600° C.

B.—*Reduction temperature series:* Six- to 8-mesh samples were reduced essentially completely at 450°, 500°, 550°, 600°, and 625° C and tested in the synthesis. Particles of 28- to 32-mesh were completely reduced at 450° and 600° C. Most of the tests were made without sieving catalyst after pretreatment.

C.—*Extent of reduction series:* To ensure uniform reduction throughout the catalyst bed, 6- to 8-mesh particles were reduced at 400° C; at this temperature the rate of reduction is low. Catalysts were not sieved after pretreatment.

The geometry of the reduced catalyst per gram of raw (unreduced) catalyst may be described as follows:

1. Hypothetical spherical radius:

Mesh size:	*Particle radius, R, cm*
4–6	0.151
6–8	.116
12–16	.0508
28–32	.0225
42–60	.0135

2. Properties that are independent of reduction temperature:
   a. External volume of catalyst=0.20 cc/g
   b. Pore volume=$0.089f$ cc/g, where f is the extent of reduction
   c. Porosity=$0.089f/0.20=0.445f$
   d. Depth of reduced zone from external surface $=R\{1-(1-f)^{1/3}\}$ where R is the particle radius.

3. Properties dependent on reduction temperatures:
   a. For completely reduced catalysts:

Reduction temperature, ° C:	*Surface area, m²/g*	*Average pore radius, r, A*
400	15.7	113
450	9.3	194
500	6.4	278
550	3.5	508
600	1.6	1112
625	1.6	1112

   b. For partly reduced catalysts, surface area $=S_o f$, where S_o is the area of the completely reduced catalyst.

For nitrided catalysts the same relationship holds, except that the external volume and pore volume are about 15 percent larger than for the reduced catalyst; however, to simplify calculations, the pore geometry data for reduced catalysts have been used for both reduced and nitrided samples. For nitrided catalysts of the extent of reduction series, the catalyst was reduced at 400° C to the desired extent and then nitrided in ammonia at 350° C. At this temperature ammonia nitrides only the reduced part of the catalyst and does not reduce or nitride any of the remaining magnetite.

Tables 7, 8 and 9 present activity data for the particle size, extent of reduction and temperature of reduction series, respectively. Figure 26 shows the variation of activity with particle size.

According to figure 26, activity increases rapidly with reciprocal particle radius, which is proportional to external area per gram. With increasing values of $1/R$ the slope decreases and eventually becomes zero. For catalysts reduced at 600° C, the slope apparently becomes zero at a larger particle size than for samples reduced at 450° C. These curves should become flat when the particle is sufficiently small so that the entire particle is effective.

TABLE 7.—*Variation of activity with particle size*

[Catalysts sieved after pretreatment]

Reduction temperature, ° C	Average pore radius, cm × 10^6	Particle radius, R, cm	Reduced catalysts		Nitrided catalysts		
			Extent of reduction, f	Activity, A*	Extent of reduction, f	Activity, A*	Atomic ratio, N/Fe
450	1.94	0.151	0.915	40	0.915	75	0.35
		.116	.971	54	.971	77	.40
		.0508	.977	105	.977	156	.40
		.0225	.995	185	.995	228	.43
		.0135	1.00	210	.979	222	.42
600	11.12	.116	1.00	62	† .914	† 70	.49
		.0225	1.00	76	1.00	111	.47

* Activity defined as cu cm. (STP) of H_2+CO converted per gram of iron per hour at 240° C.
† This sample not sieved.

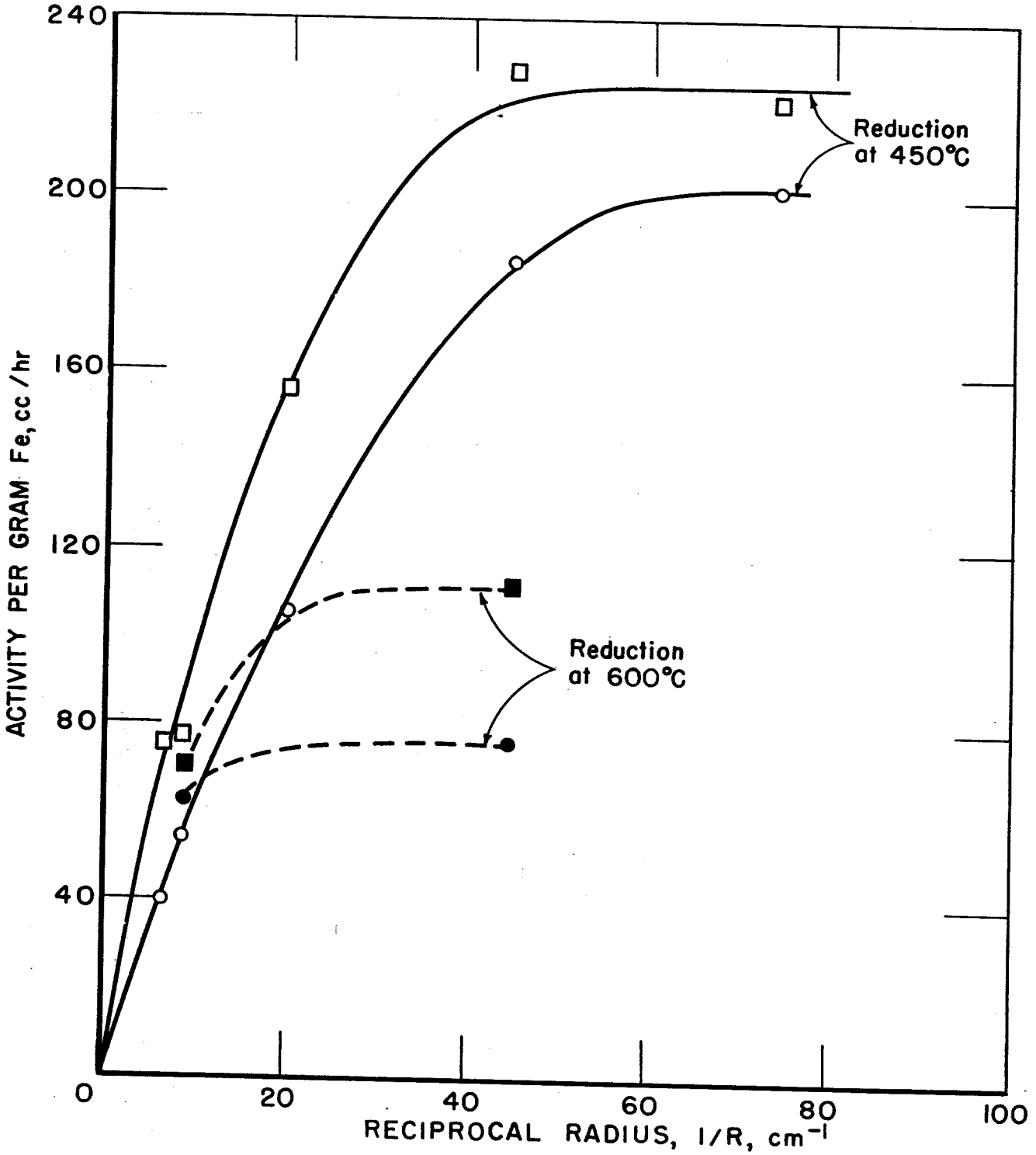

FIGURE 26.—Variation of Activity With Particle Size. Reduced catalyst denoted by circles; nitrided catalyst, squares.

TABLE 8.—*Variation of activity with extent of reduction*

[Reduction temperature=400° C, particle radius, R=0.116 cm, average pore radius, r=1.13×10^{-6} cm]

Reduced catalysts				Nitrided catalysts				
Extent of reduction, f	Depth of reduced layer × 10^2, cm	Activity		Extent of reduction, f	Depth of reduced layer × 10^2, cm	Activity		Atomic ratio, N/Fe ‡
		A *	A/f †			A *	A/f †	F
CATALYSTS NOT SIEVED AFTER PRETREATMENT								
0	0	2	----------	0	0	2	----------	0
0.082	0. 336	39	476	0. 090	0. 360	45	500	0. 48
.125	. 522	52	416	. 192	. 80	62	323	. 50
.280	1. 205	75	268	. 399	1. 82	68	170	. 41
.546	2. 67	63	115	. 577	2. 90	84	146	. 42
CATALYSTS SIEVED AFTER PRETREATMENT								
0.350	1. 57	50	143	0. 430	2. 01	55	128	0. 46
.975	8. 36	54	55	. 713	3. 94	59	83	. 39

* Activity defined as cu cm (STP) of H_2+CO converted per gram of iron per hour at 240° C.
† Activity per gram of active layer.
‡ These values give atomic ratio N/Fe for the reduced layer.

TABLE 9.—*Variation of activity with temperature of reduction* *

[Particle radius, R=0.116 cm]

Temperature of reduction, ° C.	Pore radius, $r\times10^{-6}$, cm	Reduced catalysts		Nitrided catalysts		
		Extent of reduction, f	Activity, A †	Extent of reduction, f	Activity, A †	Atomic ratio N/Fe
CATALYSTS NOT SIEVED AFTER PRETREATMENT						
450	1. 94	0. 964	73	0. 964	98	0. 42
500	2. 78	. 971	79	. 987	98	. 49
550	5. 08	. 977	69	. 964	95	. 47
600	11. 12	. 995	76	. 914	70	. 49
625	11. 12	1. 00	66	1. 00	50	. 44
CATALYSTS SIEVED AFTER PRETREATMENT						
450	1. 94	0. 977	51	0. 975	70	0. 38
600	11. 12	1. 00	62	----------	----------	----------

* Influence of temperature of reduction on smaller particles is shown in table 11.
† Activity defined as cu cm (STP) of H_2+CO converted per gram of iron per hour at 240 °C.

To estimate the magnitude of the depth of the effective catalyst layer from the external surface, a simple calculation was made assuming (1) hypothetical spherical particles, and (2) that the catalytic activity was constant in the surface layers to a depth of ΔR and was zero at depths greater than ΔR. On this basis the activity, A, is proportional to the weight of material in this active zone per unit weight of catalyst and for values of $R \geq \Delta R$

$$A=3k\frac{\Delta R}{R}\left\{1-\frac{\Delta R}{R}+\frac{\Delta R^2}{3R^2}\right\}. \qquad (31)$$

The constants k and ΔR were evaluated by a graphical method using a log-log plot of $(3\Delta R/R)(1-\Delta R/R+\Delta R^2/3R^2)$ as a function of

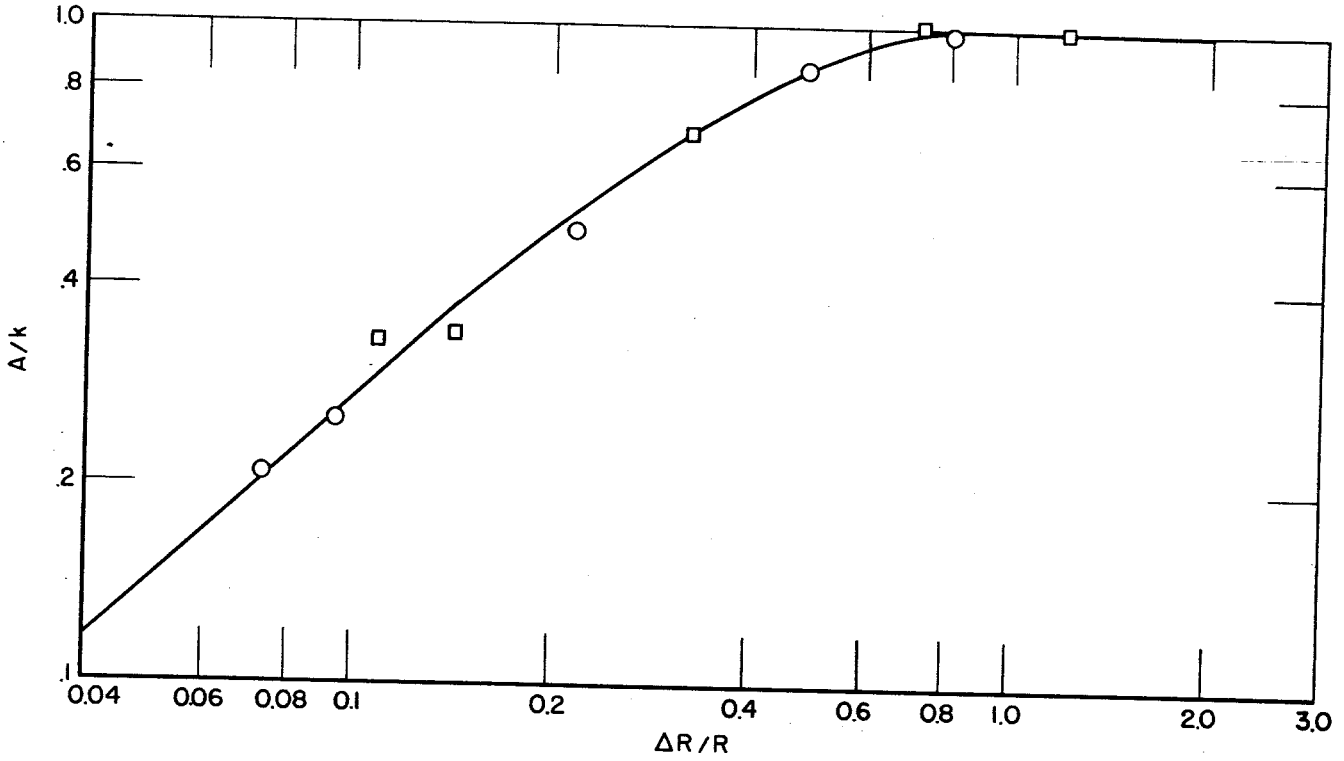

FIGURE 27.—Log-log Plot of Data for Reduced and Reduced-and-Nitrided Catalysts in Particle Size Series. ○ Represents Reduced Catalysts; □ Represents Reduced-and-Nitrided Catalysts.

$\Delta R/R$. Activity data, superimposed on the logarithmic plot in figure 27, indicate that the equation above represents the experimental results satisfactorily. The values for the constants were

Catalyst	Reduction temperature, ° C	ΔR, cm	k
Reduced	450	0.0110	211
Nitrided	450	.0175	221
Reduced	600	.05	76
Nitrided	600	.03	110

The values of reduction at 600° C, based on only two points each, are shown only to illustrate the direction of change in these parameters with increasing reduction temperature. It should be noted that ΔR is an average depth of useful catalyst for a hypothetical system in which the activity is constant in the effective zone and is zero beyond this depth. Actually the effectiveness decreases rapidly with distance from the surface, as shown in table 8 for the extent of reduction series; however, the quantity ΔR is useful in discussing the data in a simple manner. With reduced catalysts the activity ceased to increase at an extent of reduction of about 28 percent, corresponding to a depth of reduced layer of 0.012 cm in good agreement with values above; however, for nitrided catalysts this depth must be taken as 0.026 cm. These values should be regarded as tentative, being based on catalysts that were not sieved after pretreatment.

In the reduction temperature series (table 9) for 6- to 8-mesh reduced catalysts no definitive change in activity was observed, although the average pore radius increased fivefold and the surface area decreased correspondingly. For nitrided catalysts activity was constant for reduction temperatures at 450° to 550° C, but decreased significantly for 600° and 625° C. As the pore geometry of catalysts reduced at 600° and 625° C was essentially identical, the lower activity at the higher temperature cannot be attributed to a smaller surface area. With 28- and 32-mesh catalysts a marked decrease in activity was observed for both reduced and nitrided catalysts when the reduction temperature was increased from 450° to 600° C, as shown below:

Reduction temperature, ° C	Activity of catalyst, A, cu cm/g Fe-hr at 240° C	
	Reduced	Nitrided
450	185	228
600	76	111

In the medium-pressure synthesis at the temperatures used in the present study the pores of iron catalysts are filled with liquid hydrocarbons (*53*), and mass transfer involves dissolution in and diffusion through liquid films and liquids in pores. From the data of tables 7, 8 and 9, this summary relating to catalyst geometry is made:

Variable	*How varied*	*Variation of activity*
1. External area	Particle size	Large
2. Area of pore openings.	Particle size	Large
3a. Surface area	Reduction temperature	Slight
3b. Surface area	Extent of reduction	Large
4. Pore volume	Extent of reduction	Large
5. Average pore radius.	Reduction temperature	Slight
6. Depth of pores	Extent of reduction	Large

The general aspects of items 1, 2, 3a and 5 could be explained by assuming that the slow step is the rate of dissolution and diffusion of the reactants through oil films at the external surface of the particle; however, the large variations in 3b, 4 and 6 require a more complicated mechanism, probably involving diffusion in oil-filled pores coupled with reaction at the catalyst surface.

The present results indicate that the average depth of effective catalyst on the periphery of the particle is of the order of 0.01 to 0.02 cm for samples reduced at 400° and 450° C and for samples reduced at 600° C of the order of 0.04 cm. Thus, the average depth of effective catalyst increases with increasing pore radius. For larger particles the increase of effective depth appears sufficient to compensate rather exactly for the decreased surface area, and the rate remains essentially constant as the temperature of reduction is increased from 450° to 550° C. For smaller particles a sufficient depth of effective catalyst is apparently not available to compensate for the decrease in surface area as the reduction temperature was increased from 450° to 600° C.

A generalized picture of catalyst pores during synthesis is proposed, based on the data presented, and these hypotheses were examined with respect to selectivity of the catalysts and changes of catalyst composition that occur during synthesis. A typical simplified pore as shown in figure 28 is filled with liquid hydrocarbon, and the average and ultimate depths of active layer are shown by dotted lines. Hydrogen and carbon monoxide dissolve in the liquids and diffuse into the pore; the concentration gradients that cause diffusion are produced by the reaction on the walls of the pores. Synthesis products—water, carbon dioxide, and hydrocarbons—dissolve in the liquid hydrocarbons in the pore and diffuse to the pore mouth. As the solubilities of gaseous

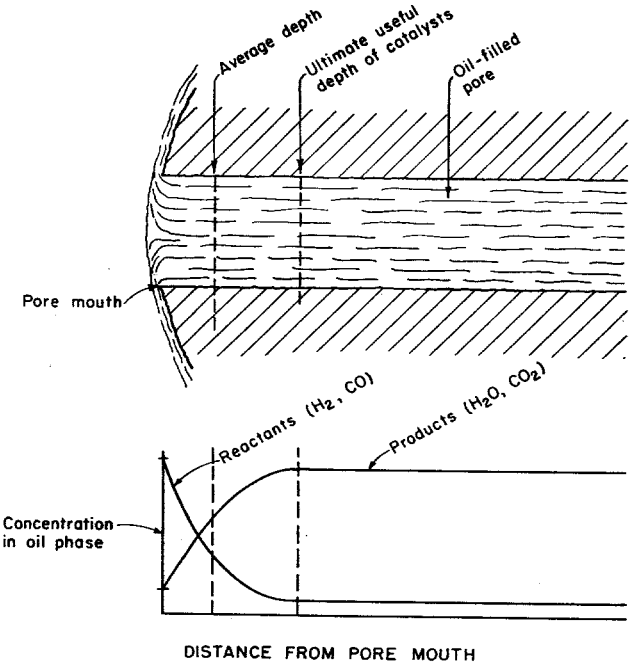

FIGURE 28.—Schematic Representation of a Pore in a Fischer-Tropsch Catalyst.

hydrocarbons, water and carbon dioxide in liquids exceed those of the reactants, it is not necessary to postulate the presence of a gas phase within the pores. High molecular weight liquids produced in the pore cause a small net flow of liquids out of the pore.

The concentrations of hydrogen and carbon monoxide, as shown by a single curve in figure 28, decrease rapidly with increasing distance from the pore mouth from values in equilibrium with the gas phase until the concentration is sufficiently low so that the rate is zero due to either kinetic or thermodynamic limitations. The concentrations of water and carbon dioxide increase from values in equilibrium with the gas phase to high constant values at the point where the concentration of reactants becomes so low that synthesis does not occur. On this basis optimum conditions for oxidation of iron are found in the interior of the particle beyond the effective depth, and optimum conditions for formation of carbide and free carbon occur in the effective layer.

In the present experiments with $1H_2+1CO$ gas carbon monoxide is used in greater amounts than hydrogen (the overall usage ratio of H_2 to CO is about 0.7); thus the liquid hydrocarbons in the pores in the ineffective portion of the catalyst should contain sizable quantities of dissolved hydrogen, as well as dissolved water, carbon dioxide, and light hydrocarbons. In the ineffective zone, hydrocracking reactions leading to a decrease in molecular weight may occur.

In the experiments described in tables 7, 8 and 9, representative samples of the entire

catalyst charge were taken after 6 weeks of synthesis. After extraction to remove adsorbed hydrocarbons, entire particles were analyzed for iron, carbon, nitrogen, and oxygen, and the changes in concentration of oxygen, carbon, and nitrogen are expressed as differences of atom ratios with respect to iron. For all of the experiments, the changes in atom ratios are divided by the initial extent of reduction.

In the next section it will be shown that the depth of effective catalyst is approximately proportional to the average pore radius. On this basis the ratio of total pore length (particle radius or depth of reduced zone) to average pore radius was taken as a measure of the relative amounts of ineffective and effective catalyst, and the selectivity and composition change data are plotted against this quantity.

Despite a number of complicating factors, the data show the following trends as the ratio of ineffective to effective catalyst was increased: (1) The oxidation of the catalyst increased, (2) the deposition of carbon and elimination of nitrogen (if present) decreased, and (3) the average molecular weight of the product decreased. Data for the temperature of reduction series in figure 29 are shown as an example of composition changes.

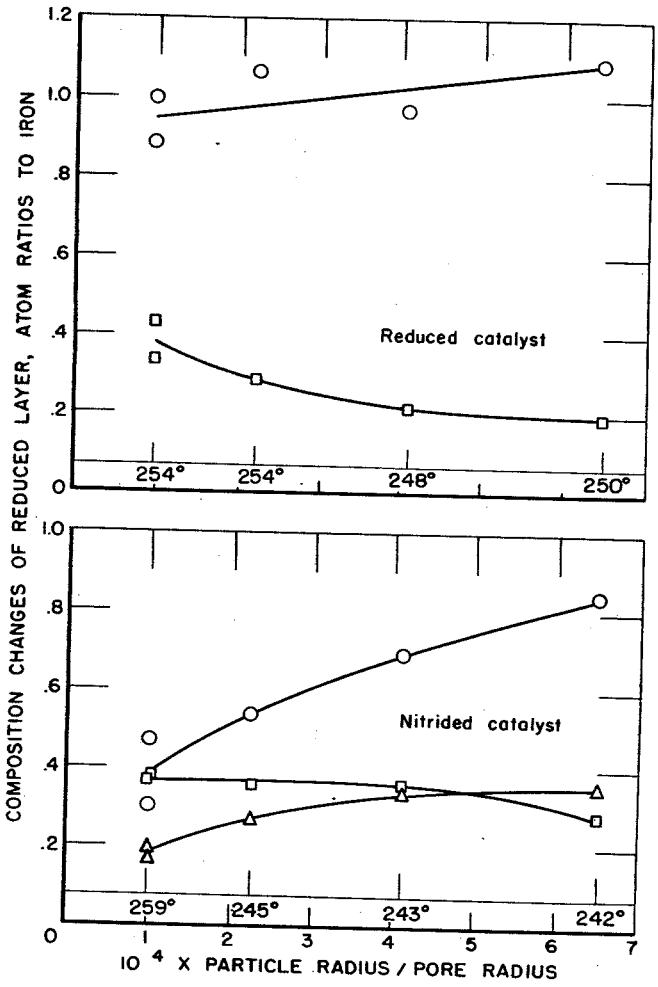

FIGURE 29.—Changes in Catalyst Composition in 6 Weeks of Synthesis Expressed as Change of Atom Ratios to Iron of Oxygen (○), Carbon (□), and Nitrogen (△), Divided by Extent of Reduction, *f*, as a Function of Particle Radius Divided by Average Pore Radius for Reduction Temperature Series. Synthesis temperatures are shown on graphs.

The present postulates provide qualitative explanations for a number of observations on the Fischer-Tropsch synthesis at temperatures below about 290° C:

1. As synthesis temperature is increased, the depth of the effective layer should decrease, and this is consistent with available data showing that the rate of oxidation of the catalyst increases and the average molecular weight of the product decreases with increasing synthesis temperature.

2. The activity and selectivity of reduced or nitrided fused catalysts (*4*, *8*, *53*, *55*) remains essentially constant for long periods, although the composition of the catalyst changes drastically. For example, the percentage of iron as oxide in reduced catalysts increases from zero to 80 in 6 weeks of synthesis at 21.4 atmospheres. These data can be explained by the postulate that the catalyst oxidizes predominantly at the interior of the particle.

3. Surface layers of activated steel lathe turning (*12*) and steel spheres, a thickness of active material of about 0.006 cm on a core of massive iron, oxidized very much more slowly than fused catalyst, despite the fact that the massive iron catalysts were operated at temperatures as high as 290° C compared with a maximum of 270° C for fused catalysts.

These postulates certainly will not explain all aspects of the synthesis. The relative rates of reactions for chain growth, chain termination, and hydrocracking probably do not increase at the same rate with increasing temperature, and the rates of reactions with the catalyst, such as oxidation and carburization, probably increase with increasing temperature. Hydrocracking reactions probably do not occur to a significant extent on iron catalysts (*34*).

APPLICATION OF A MODIFIED WHEELER EQUATION

The preceding section presented data for the variation of the rate of the Fischer-Tropsch synthesis with catalyst geometry. Calculations based on a simplified model indicate that average depth of effective catalyst extends only 0.01 to 0.04 cm from the external surface. In this section equations based on a more realistic model, in which diffusion and reaction in cata-

lyst pores are considered, are applied to the synthesis data (*3*).

A special solution of the differential equation of Wheeler (*68, 69*) was derived on the assumption that the particles are spheres and that the synthesis is a simple first-order reaction. The synthesis, to at least a first approximation (*8, 60*) is first-order with respect to the partial pressure of synthesis gas.

Wheeler's differential equation (*68, 69*) for spherical particles is

$$\frac{d^2C}{dx^2}+\frac{2}{x}\frac{dC}{dx}=b^2C \qquad (32)$$

where C=concentration of reactants at distance x from center, $b=2(k/\bar{r}D)^{1/2}$, k=first-order rate constant, $\bar{r}$=average pore radius, and D=diffusivity. Equation (32) was solved for particles in which a layer of porous, active iron of depth $R-r$ (fig. 30) is formed on a core of inert magnetite by reduction. The following limiting conditions were used: $dC/dx=0$ at $x=r$, where $0\leq r\leq R$, and $C=C_0$ at $x=R$, where C_0 is concentration at pore mouth, to yield

$$\left(\frac{dC}{dx}\right)_R=C_0b\left[\frac{\cosh(R-r)b+rb\sinh(R-r)b}{\sinh(R-r)b+rb\cosh(R-r)b}-\frac{1}{bR}\right]$$
$$=C_0bX. \qquad (33)$$

For porous catalysts in which the total surface area greatly exceeds the external area of the particles, the productivity per gram of iron, A, equals the product of the area of pore openings at the external surface times the rate of diffusion at this interface.

$$A=\frac{3V_GD}{2R}\left(\frac{dC}{dx}\right)_R=\frac{3VD_GC_0bX}{2R}=\frac{3V_GC_0}{R}\left(\frac{kD}{\bar{r}}\right)^{1/2}X. \qquad (34)$$

Here V_G is the pore volume for the completely reduced catalyst per gram of iron. V_G is used only to define the ratio of the area of pore mouths to total external area which is equal to the porosity for a completely reduced catalyst (*3*). The porosity of the reduced portion of the catalyst is independent of the extent of reduction, f, for $f>0$, and is most simply defined in terms of the completely reduced catalyst.

For a graphical determination of the constants of equation 34, the following transformations are made: A quantity, L, the "depth factor," is defined as $L=(R-r)b$; $r=ZR$, then $L=bR(1-Z)$, $bR=L/(1-Z)$, and $br=LZ/(1-Z)$; Z is related to extent of reduction f by

$$Z=r/R=(1-f)^{1/3}.$$

Then the expression for X in equation (33) may be written as

$$X=\frac{\cosh L+\frac{LZ}{1-Z}\sinh L}{\sinh L+\frac{LZ}{1-Z}\cosh L}-\frac{1-Z}{L}. \qquad (35)$$

Equation (34) becomes.

$$Y=\frac{AR\bar{r}^{1/2}}{3V_GC_0}=(kD)^{1/2}\times X. \qquad (36)$$

The value of L is given by

$$L=\frac{2R(1-Z)}{\bar{r}^{1/2}}\left(\frac{k}{D}\right)^{1/2}=L'\left(\frac{k}{D}\right)^{1/2}. \qquad (37)$$

Logarithmic plots of X (equation (35)) as functions of L and Z are presented in figure 31. All of the terms in Y and L can be evaluated in terms of measured quantities except k and D, and these quantities can be estimated from the values required to yield the best fit of experimental data in figure 31. Also plotted on this graph as dotted lines are the variations of X, as $L=bR(1-Z)$ is varied by changing the quantity of Z at constant values of bR of 0.5, 1, 2, 5, and 10. These lines indicate how the activity should vary with the extent of reduction.

In tables 7, 8, and 9 of the preceding section, activity data were presented for reduced and reduced-and-nitrided fused iron catalysts for changes in particle size, extent of reduction, and temperature of reduction. These experiments were made at different temperatures near 240° C, and the activity data were corrected to 240° C using the Arrhenius equation with an activation energy of 19 kcal/mole (*54*). Subsequent work showed that this activation energy was valid only for 6- to 8-mesh and larger particles; hence activation energies were determined as a function of particle size.

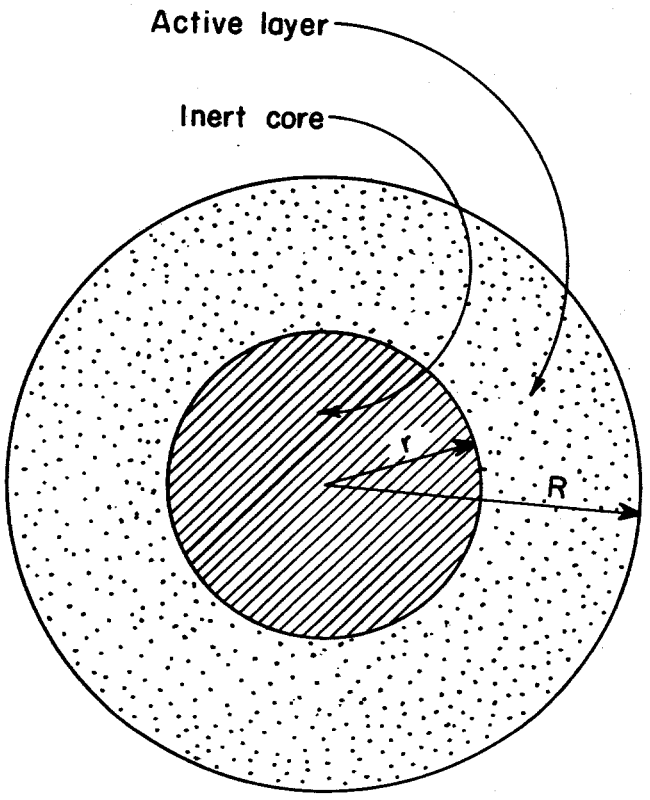

FIGURE 30.—Idealized Representation of Partly Reduced Particle of Catalyst.

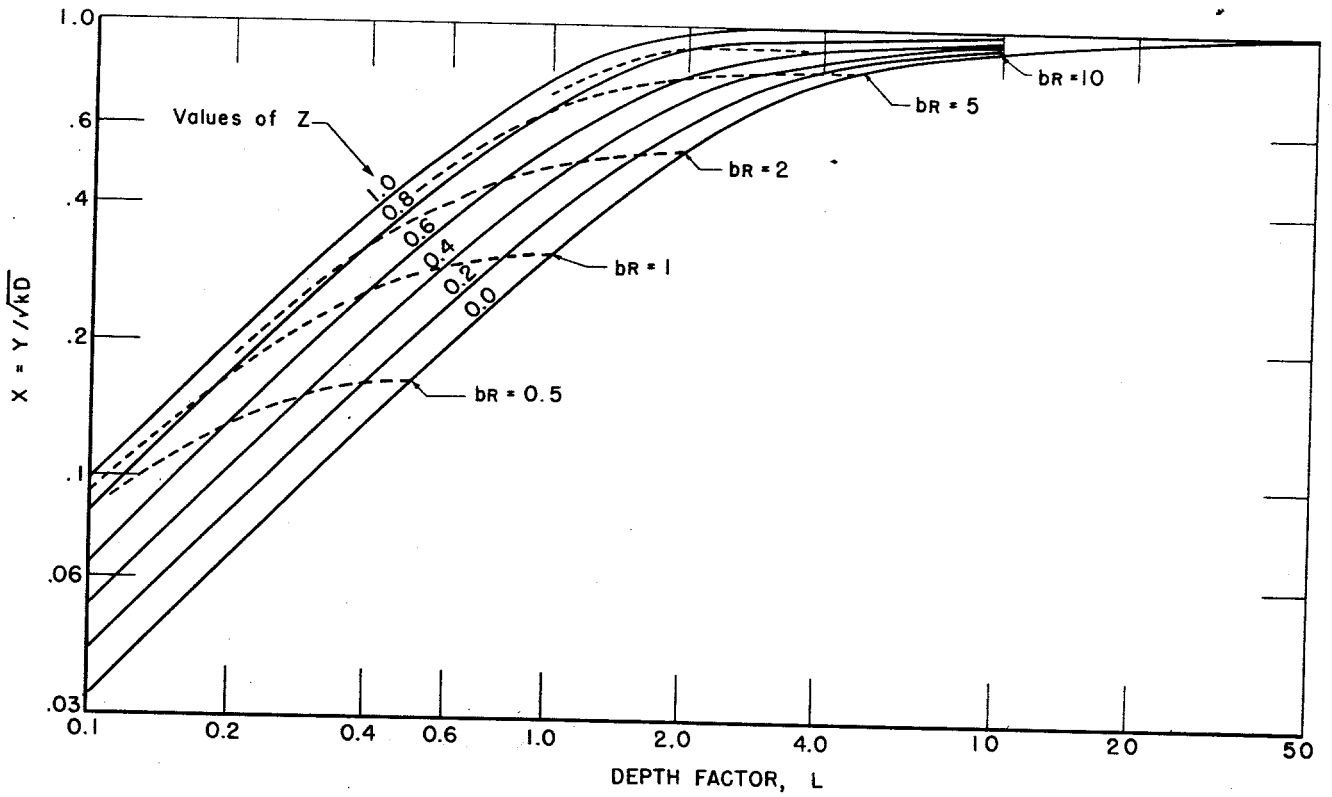

FIGURE 31.—Logarithmic Plots of Equation (34).

Experiments were made on three samples of nitrided iron catalyst D3001, sieved after reduction at 450° C and nitriding to yield particles with average hypothetical spherical radii of 0.116, 0.0508, and 0.0225 cm. Tests were made with $1H_2+1CO$ gas at 21.4 atmospheres after about 2 weeks of synthesis. The observed activation energies determined by least squares evaluation of the data were 20.1, 27.0 and 27.6 kcal/mole for catalysts with average particle radii of 0.116, 0.0508, and 0.0225 cm, respectively.

Wheeler's simplified equation (58)(*68*) was differentiated to obtain $E_{obsd}=R\ \mathrm{d}\ ln\ A/\mathrm{d}(1/T)$, where E_{obsd} is the observed activation energy. From the resultant equations, E_{obsd}/E_t—where E_t is the activation energy at the surface—may be plotted as a function of R on double logarithmic scales to provide a curve for obtaining E_t and extrapolation. The activation energies are given in table 10; the value of E_t was 28.0 kcal/mole.

TABLE 10.—*Activation energies as a function of particle size for nitrided iron catalysts.*

Mesh size	Particle radius, cm	Activation energy, kcal/mole
4–6	0.151	* 18.6
6–9	.116	20.1
12–16	.0508	27.0
28–32	.0225	27.6
42–60	.0135	* 28.0

* Obtained by extrapolation.

Equation (34) requires that the productivity, A, be known at a constant value of reactant concentration, C_0. The productivity was calculated at zero conversion of reactants, where C_0 equals the concentration of reactant in the feed. For this purpose the well-tested empirical equation (*8*, *31*), $-ln(1-x)=k'/Q$, was used, where x is the fraction of hydrogen plus carbon monoxide reacted, Q is the feed rate in cubic centimeters (STP) of hydrogen plus carbon monoxide per second per gram of iron, and k' is a rate constant. At zero conversion the volume in cubic centimeters (STP) of gas converted per second per gram of iron equals k' (*31*). The value of k' was then corrected to 240° C using the appropriate activation energy.

For series B and series C (p. 30) using 6- to 8-mesh particles an activation energy of 19 kcal/mole was used. For series A (p. 30) with both reduced and nitrided catalysts activation energies in table 10 were used. Productivity, A, is defined here as cubic centimeters (STP) of hydrogen and carbon monoxide consumed per second per gram of iron at 240° C and zero conversion, and concentration, C_0, is expressed as volumes (STP) of hydrogen plus carbon monoxide per unit volume.

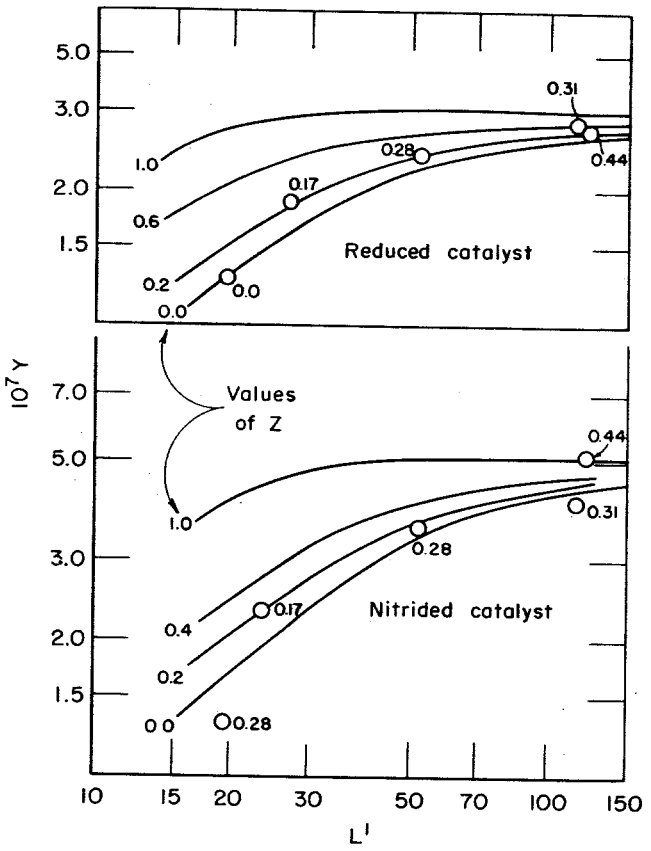

FIGURE 32.—Data for Particle Size Series Superimposed on Curves of Figure 31.

An idealized model of catalyst geometry was used, and the average catalyst properties were obtained by gross measurements: equivalent spherical particle radii from particle density and the average weight of 100 particles, average cylindrical pore radii from surface area and pore volume, and depth of reduced layer from extent of reduction. Assumptions of the model and the methods of averaging may lead to moderately large discrepancies in some cases. In view of these factors, experimental uncertainties, and the method used in fitting data to theoretical curves (super-position of log-log plots), the reliability of values obtained for constants is not high.

Fair agreement of data from the particle size series and extent of reduction series with curves of figure 31 was obtained, as shown in figures 32 and 33. In fitting experimental data to the theoretical curves, logarithmic plots of experimental results in terms of Y and L' were superimposed on figure 31. As these plots have an additional parameter Z, each experimental point should fall on the theoretical curve for the appropriate value of Z. In figures 32 and 33 the values of Z are given for each experimental point, as well as the theoretical curves for different values of Z. From the position of the experimental plot on the theoretical curves, the values of k and D may be estimated. The values of Y in these plots usually deviated less than 10 percent from the theoretical curves. Reasonable plots of data for the temperature of reduction series could not be made, as values of Y decreased rather than increased with increasing values of L'.

The values of D for nitrided catalysts of the particle size and extent of reduction series (table 11) increase with increasing average pore radius; however, the reliability of these values is too low to permit a characterization of the relationship between D and $\bar{r}$. This variation of D with $\bar{r}$ may explain why the data from the temperature of reduction series do not fit the theoretical curves in figure 31. For this series the assumption was made that $D=\gamma\bar{r}$ where γ is a constant. These data now fit the hypothetical curves in a satisfactory manner, and values of k of 8.9×10^{-8} and 7.0×10^{-8} were obtained for reduced and nitrided catalysts, respectively. The values of constant γ in table 12 justify this relationship only as a rough approximation. It is difficult to decide whether the apparent increase in diffusivity with increasing pore diameter is real or merely a correction for deficiencies of the model. Electron micrographs of replicas stripped from this catalyst after reduction at 450° or 550° C showed elongated pores with a shortest dimension of about 500 to 800 A (*46*). These and other results suggest that the catalyst has a group of larger pores that are relatively independent of reduction temperature plus smaller pores or roughness that vary sufficiently with reduction temperature to produce a tenfold change in surface area.

TABLE 11.—*Values of* k *and* D

	Reduction temperature, ° C	Average pore radius, A	Reduced catalysts		Nitrided catalysts	
			k, 10^8 cm/sec	D, 10^6 sq cm/sec	k, 10^8 cm/sec	D, 10^6 sq cm/sec
Extent of reduction	400	113	8.7	8.7	9.4	9.4
Particle size	450	194	12.4	7.0	12.0	18.8
	600	1112	----------	----------	19	75

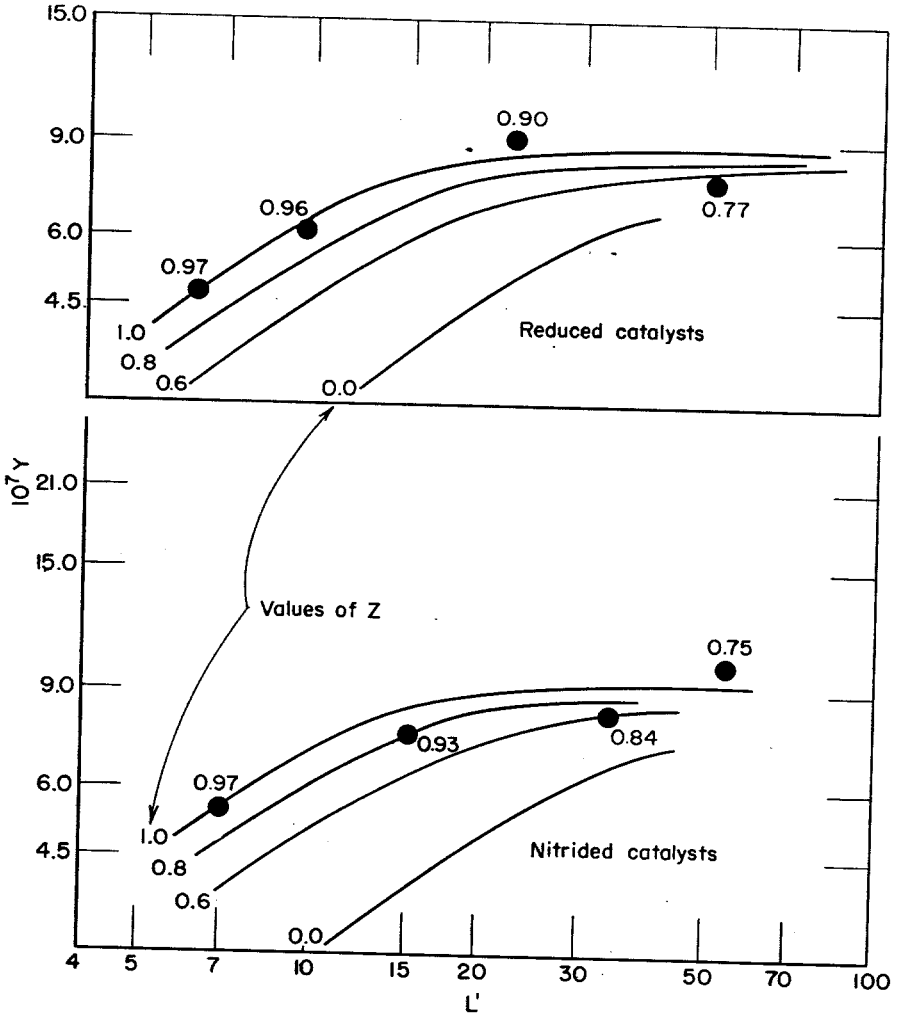

FIGURE 33.—Data for Extent of Reduction Series Superimposed on Curves of Figure 31.

Diffusivities of reactants in Fischer-Tropsch liquids have not been determined; however, estimates were made with semi-empirical equations of Wilkes and Chang (*70*) for hydrogen and carbon monoxide in a normal C_{30} hydrocarbon at 250° C using a viscosity extrapolated from the data of Rossini (*51*). These values, $D_{H_2}=1.9\times10^{-4}$ cm²/sec and $D_{CO}=1.2\times10^{-4}$, are of similar magnitude to that estimated from data of Reamer, Duffy, and Sage (*50*) for methane in white oil (molecular weight=340) $D_{CH_4}=2.0\times10^{-4}$ cm²/sec.

TABLE 12.—*Values of* $\gamma=D/\bar{r}$

	Value of γ	
	Reduced	Nitrided
Particle size:		
Reduced at 450° C	3.6	9.7
Reduced at 600° C		6.7
Extent of reduction	7.7	8.3
Reduction temperature	3.0	6.0

Eagle and Scott (*20*) found that the diffusivities of liquid hydrocarbons in silica and silica-alumina gels increased with increasing average pore radii and leveled out at the diffusivity of bulk liquid for radii of about 50 A. These data can be roughly approximated by $D=\gamma\bar{r}$ for values of $\bar{r}<40$ A. However, the diffusivities estimated from present synthesis experiments had not leveled off at the highest pore radii studied: 1,112 A. These values, 7 to 75×10^{-6} cm²/sec, are sufficiently smaller than the estimated bulk diffusivities 100 to 200×10^{-6}, so that the diffusivity-pore radius curve could flatten at the value of bulk diffusion. The observation that the diffusivity in pores is of the order of 5 to 50 percent so that in the bulk liquid may explain why diffusion in pores, but not in bulk liquid (liquid films on external surface of particles in dry-bed units and bulk liquid in oil-filled reactors) is the important slow step in the Fischer-Tropsch synthesis, at least at temperatures below about 290° C.

Kölbel (*35*) determined solubilities of gases in Fischer-Tropsch wax. At 233° C the solubilities were: H_2, 0.17; CO, 0.20; CO_2, 0.44; and H_2O, 0.73 cu cm (STP) per gram-atm. In Bureau of Mines work obtained in investigations of the oil circulation process (*12*), somewhat larger solubilities were observed in a 250° to 450° C fraction of synthesis oil at 233° C: H_2, 0.26; CO, 0.32; CO_2, 0.83; and H_2O, 0.78. In this process, synthesis plus recycle gas is passed upward through a fixed bed of catalyst submerged in synthesis oil, which is circulated upward through the bed. Apparently equilibrium was very nearly obtained at the outlet of the reactor, and solubilities during synthesis and in similar experiments with catalyst removed were essentially the same. Other studies demonstrated that about half of the normal rate of synthesis could be attained by passing synthesis gas through the cooling oil in an external absorber and circulating this oil through the catalyst bed. These results suggest that the transport of reactants through oil films external to the catalyst particles is not the rate-determining step.